Journal of Microbiological Methods 88 (2012) 117–121

Contents lists available at SciVerse ScienceDirect

Journal of Microbiological Methods

journal homepage: www.elsevier.com/locate/jmicmeth

High-throughput analysis of growth differences among phage strains

Paul E. Turner *, Jeremy A. Draghi [1], Regina Wilpiszeski

Department of Ecology and Evolutionary Biology, Yale University, New Haven, CT 06520, USA

ARTICLE INFO

Article history:
Received 22 August 2011
Received in revised form 29 October 2011
Accepted 29 October 2011
Available online 12 November 2011

Keywords:
Bacteria
Bacteriophage
Evolution
Fitness
Pseudomonas syringae

ABSTRACT

Although methods such as spectrophotometry are useful for identifying growth differences among bacterial strains, it is currently difficult to similarly determine whether bacteriophage strains differ in growth using high throughput methods. Here we use automated spectrophotometry to develop an in vitro method for indirectly distinguishing fitness (growth) differences among virus strains, based on direct measures of their infected bacterial hosts. We used computer simulations of a mathematical model for phage growth to predict which features of bacterial growth curves were best associated with differences in growth among phage strains. We then tested these predictions using the in vitro method to confirm which of the inferred viral growth traits best reflected known fitness differences among genotypes of the RNA phage phi-6, when infecting a *Pseudomonas syringae* host. Results showed that the inferred phage trait of time-to-extinction (time required to drive bacterial density below detectable optical density) reliably correlated with genotype rankings based on absolute fitness (phage titer per ml). These data suggested that the high-throughput analysis was valuable for identifying growth differences among virus strains, and that the method may be especially useful for high throughput analyses of fitness differences among phage strains cultured and/or evolved in liquid (unstructured) environments.

1. Introduction

Classic studies with bacteria and lytic phage helped establish the field of molecular biology (Davis, 2003), and recent efforts show that these microbes can usefully address questions in evolutionary biology (Duffy and Turner, 2008; Turner et al., 2009). Growth of lytic phage is traditionally visualized via plaques formed on superabundant host lawns in semi-solid agar, and growth performance of phage genotypes can be quantified by manually counting plaques to gauge changes in virus number (titer per volume) over time. However, this traditional method is labor-intensive and potentially subjective, perhaps constraining the scale and ambition of evolution experiments using phage. Some bacteria studies have complemented the analogous procedure of colony counting by employing rapid, parallel quantification of bacterial growth in microplate spectrophotometers (e.g., Hegreness et al., 2006). Here we develop a new approach and supporting computer model for extending this method to efficiently infer the growth (absolute fitness) of lytic phage. We then apply the method to test for known differences in growth among phage genotypes.

Microplate spectrophotometers are generally useful for culturing large numbers of microbial samples in small volumes (e.g., in a 96-well microplate), while simultaneously obtaining measurements of the optical density of each culture. Densities of bacteria are typically estimated by scattering of light at a wavelength of 600 nm. Phage particles are too small for their densities to be quantified in this way: for example, individual virions of RNA phage ϕ6 are roughly 86 nm in diameter (Kenney et al., 1992). However, the growth of lytic phage necessarily decreases the density of their sensitive host bacteria, and, in well-mixed liquid culture, phage can drive their hosts to extinction. If phage and superabundant bacteria are cultured together in a microplate well, spectrophotometry can be used to track host density as it initially increases, peaks as the phage infect and lyse their hosts, and finally decreases when hosts are forced to extinction. Clearly, the shape of such a host–density curve must be influenced by the intrinsic growth ability of a phage genotype, but the nature of this relationship is not obviously informative.

Here we present a computer model of lytic phage infection of an exponentially growing culture of host bacteria to demonstrate how host–density curves may be translated into quantitative measures of phage growth. To confirm predictions of our model we examined infection of *Pseudomonas syringae* pathovar *phaseolicola* bacteria by genotypes of phage ϕ6, strains which differed in performance gauged through the traditional fitness assay (Chao, 1990).

2. Materials and methods

2.1. Strains and culture conditions

P. phaseolicola was purchased from American Type Culture Collection (ATCC #21781), and cultured at 25 °C in LC medium: Luria–Bertani broth at pH 7.5 (Turner and Chao, 1998). Overnight cultures of

* Corresponding author. Tel.: +1 203 432 5918; fax: +1 203 432 5176.
E-mail addresses: paul.turner@yale.edu (P.E. Turner), jdraghi@gmail.com (J.A. Draghi), ginawilp@gmail.com (R. Wilpiszeski).
[1] Current address: Department of Biology, University of Pennsylvania, Philadelphia, PA 19104, USA.

0167-7012/$ – see front matter © 2011 Elsevier B.V. All rights reserved.
doi:10.1016/j.mimet.2011.10.020

bacteria were grown from a single colony placed in 10 ml LC medium, with shaking incubation (120 rpm). Bacterial stocks were stored in 4:6 glycerol/LC (v/v) mixtures at −80 °C.

All viruses were derived from wild type phage ϕ6 (ATCC #21781-B1). An earlier experiment allowed three lineages of the virus to evolve at Low (L) and High (H) multiplicity-of-infection (MOI, ratio of viruses to cells; Turner and Chao, 1998). These six lineages are abbreviated as L1, L2, L3, and H1, H2, and H3, respectively. After 300 generations of virus evolution, 10 clones were isolated at random from each of these six populations (Montville et al., 2005). Experiments confirming simulation predictions (see Results) used 24 of these 60 strains, and data are reported for assays involving 12 of the clones (PT604[L1.2], PT609[L1.7], PT611[L1.9], PT612[L1.10], PT616 [L2.4], PT624[L3.2], PT630[L3.8], PT635[H1.3], PT644[H2.2], PT652 [H2.10], PT653[H3.1], and PT657[H3.5]; Montville et al., 2005).

Virus lysates were grown by mixing phage and a 200-μl lawn of stationary-phase bacterial culture in 3 ml of LC top agar (0.7%) overlay on LC solid agar (1.5%). After 24 h, plaques were collected by placing the top agar layer in 3 ml LC, gently vortexing to break apart plaques, and filtering (0.22 μm filter, Durapore, Millipore) the supernatant to remove bacteria. The resulting phage lysate was stored at −20°C in a 4:6 glycerol/LC (v/v) mixture. The titer (density) of a phage lysate was determined by enumerating plaques visualized via dilution series plated on *P. phaseolicola* lawns, where each plaque was assumed to be initiated by a single phage particle. Thus, lysate titers are plaque-forming units (pfu) per ml.

2.2. Estimating phage growth

A 200-μl volume containing 4×10^7 stationary-phase bacterial culture and 400 pfu of test phage (initial MOI of 1×10^{-5}) was placed in each well of a transparent, flat-bottomed, 96-well microplate (Corning Inc., Corning, NY). The microplate was incubated at 25 °C with orbital shaking in a Tecan (Mannedorf, Switzerland) model Infinite F500 spectrophotometer. Optical density at 600 nm wavelength (OD_{600}) was measured for each well at 4 min intervals; measurements were obtained for at least 10 h to ensure that bacteria went extinct.

A script was written and executed in R to smooth each OD_{600} curve and to estimate N_{max} (maximum bacterial population size) and t_{ext} (time at which bacteria become extinct). Curves were smoothed by averaging each point with its immediate neighbors, and N_{max} was the highest smoothed value. In theory, t_{ext} could be calculated as the time when the OD_{600} reading first returns to its initial level. However, this approach would be sensitive to anomalies caused by contents of lysed cells, small quantities of resistant cells, and/or contaminants. Also, inner-lid condensation on a microplate may inflate OD measures at times less than ~1 h, making initial OD_{600} readings unreliable. To measure t_{ext} more accurately, we used the first time point which was more than 80 min after the peak OD_{600}, and which differed by less than 0.002 from the preceding measurement. This heuristic was chosen to give consistent and sensible results for a wide range of curves (data not shown).

To estimate the number of phage produced in a well at the end of the assay $P(t_{ext})$, the microplate was placed in a swing-bucket of an Eppendorf (Hamburg, Germany) model #5810 centrifuge, and spun for 10 min at 6000 rpm to pellet any remaining cells. Then, diluted samples of supernatant were plated on bacterial lawns to achieve non-overlapping plaques (i.e., ~200 plaques per plate maximum), allowing estimates of $P(t_{ext})$. Eq. (5) was then used to calculate r for each strain using $P(t_{ext})$, initial phage concentration, and t_{ext}.

3. Results

3.1. Phage growth simulations

Our initial goal was to predict which features of host–density curves were best associated with phage growth, and to assess how these associations changed with respect to variation in phage fitness components (growth-associated virus traits). Thus, we developed a model for phage growth in an expanding population of susceptible bacterial hosts. In the model, phage attached to bacteria with second-order kinetics, reproduced within host cells for a specified time, and then lysed the cells to release progeny phage that continued the infection process. A specific phage phenotype was characterized by three parameters: rate of virus attachment to cells (α), burst size (virus particles produced per infected cell; β), and burst time (i.e., latent period, the time between cell attachment and cell lysis; τ). Previous models of phage growth have focused on these same parameters to study variation, evolution and optimality in phage 'life-histories' (Abedon, 1989; Abedon et al., 2001; Bull, 2006; Wang, 2006). Studies with phage ϕ6 (Dennehy and Turner, 2004; Dennehy et al., 2007) and other phage types (e.g., Abedon et al., 2003; Wang, 2006; Heineman and Bull, 2007) have also ascribed relative differences among genotypes across the lytic life-cycle to differences in burst time and burst size.

To simplify our model we ignored several phage characteristics that were expected to account for relatively little variation in fitness (relative growth) among strains of phage ϕ6. We assumed that phage did not decay (become nonviable for infection) during the simulations, which generally lasted for less than 24 h. This assumption is justified for phage ϕ6, which remains viable in the absence of cells for several days at 25 °C in the standard culture medium (O'Keefe and Turner, unpublished results; see also McBride et al., 2008). Our model follows other studies in assuming that infected cells immediately stop growing and are immune to further infection (e.g., Wang, 2006). The consequences of these assumptions are discussed below.

The dynamics of our model can be described as a system of three differential equations:

$$\begin{aligned} dS/dt &= r_s S - \alpha SP \\ dI_t/dt &= \alpha SP \\ dP/dt &= I_{t-\tau} - \alpha SP \end{aligned} \qquad 1\text{–}3$$

where S is density of susceptible hosts, I_t is density of infected hosts at time t, P is density of free phage particles, α is attachment rate in units of ml cell·phage $\min^{-1}$, β is burst size in pfu, τ is burst time in min, and r_S is intrinsic rate of increase of susceptible hosts. These equations model a well-mixed phage/bacteria community with ample space and nutrients for bacterial growth. The equations are similar to those of Wang (2006), without the assumption of logistic bacterial growth.

Using Eqs. (1–3), we numerically simulated a phage inoculum introduced into a growing bacterial culture. In each simulation, 400 pfu were mixed with 4×10^7 bacterial cells (MOI $=1\times10^{-5}$) in a volume of 1 ml. Details of the simulation method are presented in the Appendix. Fig. 1(a)–(c) shows simulated curves with varying burst times, burst sizes, and rates of attachment. Since a spectrophotometer cannot discriminate between infected and susceptible hosts, we plotted the total bacterial density $N(t)$:

$$N(t) = S(t) + \sum_{i=t-\tau}^{t} I_i. \qquad 4$$

Each $N(t)$ curve showed a similar pattern: the host population increased exponentially for several generations, then briefly reached a plateau before crashing when the phage population overwhelmed the host population. Fig. 1(d) plots both host and phage densities over time, illustrating the fundamental asymmetry between bacterial and phage growth dynamics. The simulated bacterial hosts increased steadily at a slow rate, reflecting cell reproduction via binary fission and short generation times. In contrast, phage reproduced in large bursts after a longer generation time. Due to these dynamics, and the very low starting MOI, the phage particles were significantly

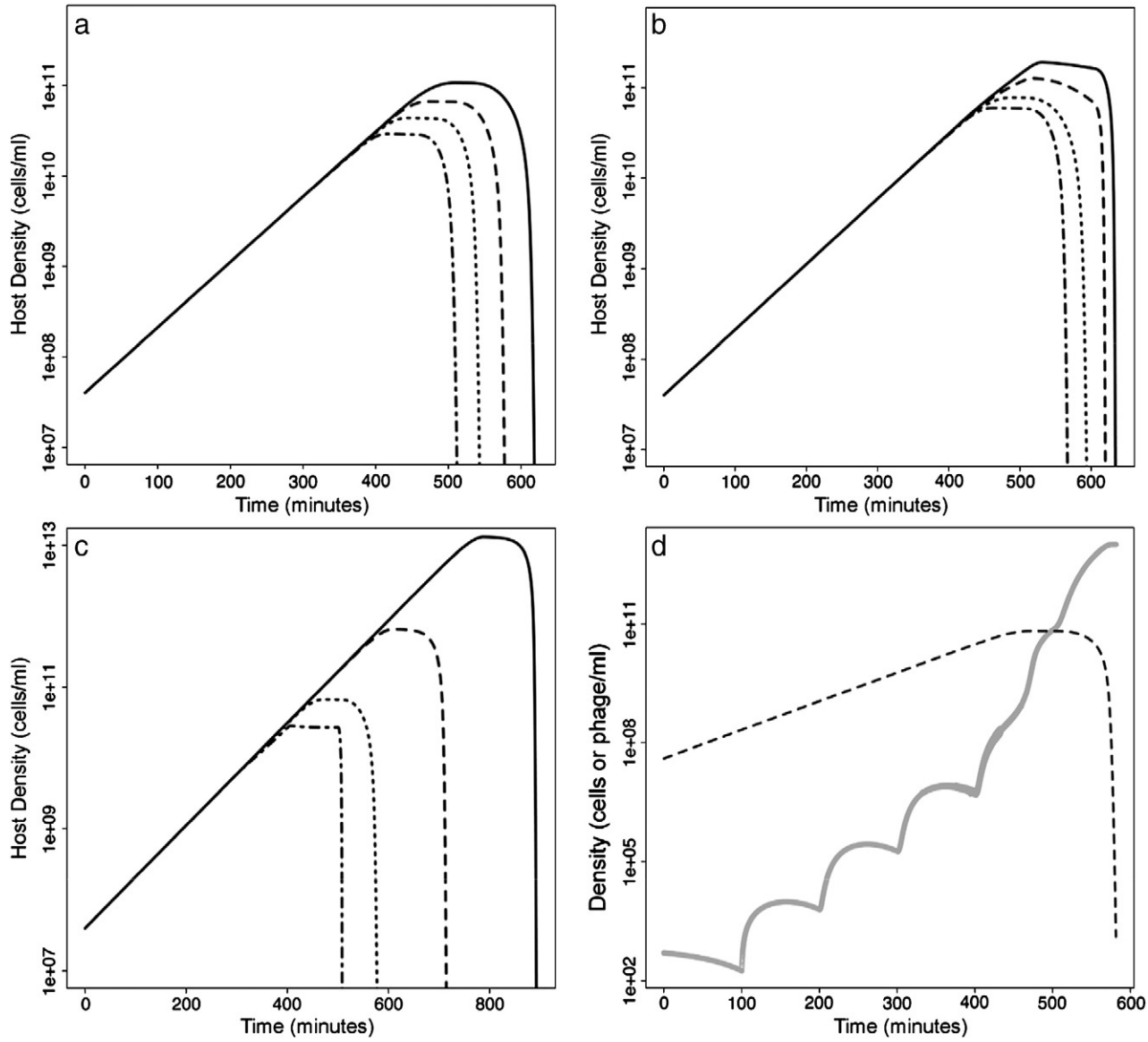

Fig. 1. Simulated host–density curves showing the dynamics of host growth and phage infection. a) Variation in burst time: solid line, $\tau = 105$ min; dashed line, $\tau = 100$ min; dotted line, $\tau = 95$ min; dot–dash line, $\tau = 90$ min. Other parameters are $\alpha = 1 \times 10^{-10}$, $\beta = 150$. b) Variation in burst size: solid line, $\beta = 100$; dashed line, $\beta = 120$; dotted line, $\beta = 140$; dot–dash line, $\beta = 160$. Other parameters are $\alpha = 1 \times 10^{-10}$, $\tau = 100$. c) Variation in attachment rate: solid line, $\alpha = 1 \times 10^{-12}$, dashed line, $\alpha = 1 \times 10^{-11}$, dotted line, $\alpha = 1 \times 10^{-10}$, dash–dot line, $\alpha = 1 \times 10^{-9}$. Other parameters are $\beta = 150$, $\tau = 100$ min. d) Phage growth during a simulation with $\alpha = 1 \times 10^{-10}$, $\beta = 150$, and $\tau = 100$ min. The dotted line plots host density, while the gray line displays the concentration of free phage on the same scale.

outnumbered by their host cells for most of the simulation. This pattern justifies ignoring any co-infection events that may have occurred (and readily occur at conditions of MOI $\gg$ 1.0 in phage ϕ6; Froissart et al., 2004), as well as growth of infected cells; both phenomena would be relevant for only a small portion of the total experiment.

Fig. 1(a)–(c) demonstrates that variation in each of the three life-history characteristics changes the size of the curve for bacterial growth, without altering its basic shape. Specifically, increased attachment rate, increased burst size, and decreased burst time, all led to reduced t_{ext} and lowered N_{max}. In the absence of trade-offs between virus traits, these same directional changes should each increase the growth ability of a phage phenotype. Our simulated infections, therefore, suggested that N_{max} and t_{ext} should be negatively associated with phage growth (absolute fitness).

To confirm these relationships, we simulated the growth of 500 hypothetical phage strains with random life-history parameters. For each strain, $\ln(\alpha)$ was drawn uniformly from the interval $[-26, -18)$, β was selected uniformly from the interval [50, 300), and τ was drawn uniformly from the interval [80, 150). These ranges were chosen to bracket measured values for phage ϕ6 strains (e.g., Dennehy and Turner, 2004; Dennehy et al., 2007). Absolute fitness was determined for each strain by measuring total phage at t_{ext} and calculating intrinsic rate of increase:

$$r = \frac{\ln(P(t_{ext})) - \ln(500)}{t_{ext}}. \quad 5$$

Fig. 2 plots calculated r values versus t_{ext} for the 500 strains; log-transformation of both axes reveals the relationship to be negative and approximately log–log linear. The Spearman rank correlation between these two variables was -0.995, implying that t_{ext} was a highly informative predictor of r. The Spearman correlation between N_{max} and r was -0.987, though this relationship was strongly non-linear even on a log–log plot (data not shown).

3.2. Model confirmation using growth measurements of phage genotypes

Our simulation results suggested that phage growth can be precisely inferred from apparent features of the density curves of their infected hosts. To confirm these predictions, we examined a collection of 24 previously-isolated phage ϕ6 strains (Montville et al., 2005), which differed genetically based on sequence comparisons at specific loci (Dennehy, Duffy and Turner, unpublished results; McBride et al., 2008).

The 24 clones were used in assays that estimated N_{max} and t_{ext} for each strain at initial MOI $= 1 \times 10^{-5}$. Fig. 3 shows representative examples of empirical curves for strains of differing growth ability, identifying relative values for N_{max} and t_{ext}. Using Eq. (5), we estimated r for each phage clone using its associated t_{ext} value, initial phage population size, and $P(t_{ext})$ obtained through plating assays (see Materials and methods).

Initial measurements of r for all 24 strains established a range of growth capabilities (data not shown). We then chose 12 strains representing approximately uniform intervals across this range for further study. We performed assays using these 12 strains on two separate days to control for differences between host cultures. Fig. 4 shows the calculated r values and measured t_{ext} values for these strains. Pearson correlations yielded an R^2 of 98.27% for the first day, and 99.11% for the second day. These results confirmed that t_{ext} was a precise measure of phage growth within a microplate well. The r values clearly differed between days, most likely due to differences between host cultures grown overnight from separate colony inoculations. However, we noted that the Pearson correlation between the r values for the two blocks was 0.983, indicating that t_{ext} consistently and reliably measured relative growth abilities of virus strains.

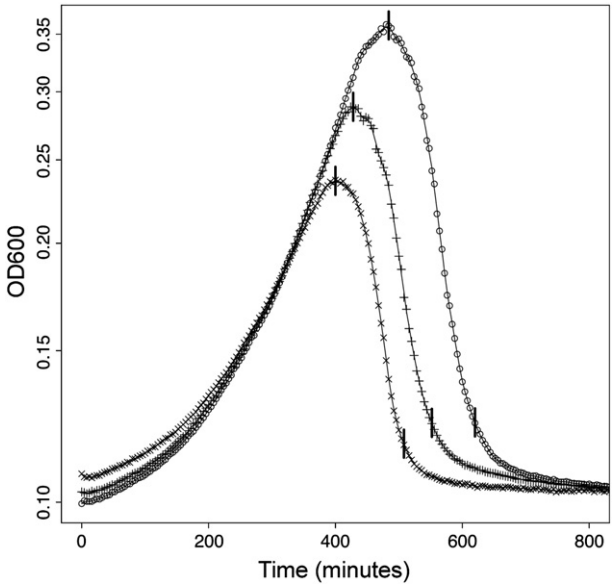

Fig. 3. Empirical curves of host density over time in three wells inoculated with different phage genotypes. Data for the wild type phage are symbolized as '×', a mildly growth-impaired genotype as '+', and a strongly growth-impaired genotype as 'O'. Points are raw measurements, and the connecting lines show the smoothed curves used to infer curve parameters. The vertical bars indicate the points classified as N_{max} and t_{ext}.

4. Discussion

In the past century, phage plaque assays were critical for discerning fundamentals in biology, including discovery of the triplet nature of the amino-acid code (Crick et al., 1961), refinement of modern cloning techniques, and use of viruses to efficiently test ecological and evolutionary theory. The size and shape of a plaque suggest how efficiently a phage variant is able to attack bacterial cells when virus infection occurs in a structured (solid) environment. Also, infections occurring in unstructured (liquid) environments can be sampled to enumerate plaque numbers per unit volume, thus estimating virus titer (density). Despite the obvious utilities of plaque-based methods, the information they yield is limited. For instance, plaque size is notoriously difficult to interpret, as it does not always correspond to a particular intra-plaque titer. Also, plaque assays are not very useful for examining intra-population variation, because differences among phage genotypes do not always translate to differing plaque morphologies. Here we presented a novel liquid-culture method for inferring differences in growth among virus genotypes. By tracking through time the effects of virus infection on

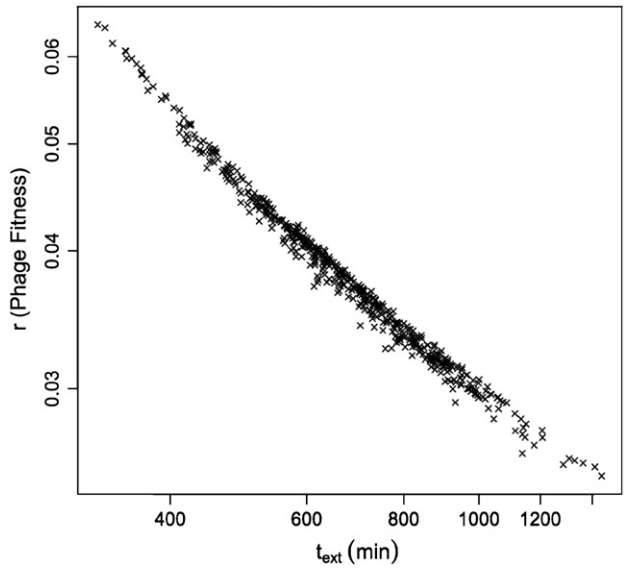

Fig. 2. The relationship between host extinction time and the calculated fitness of phage genotypes. Each simulation begins with 500 identical phage mixed with 4×10^7 host cells in 1 ml, and proceeds until the density of host cells drops below 1000 cells ml^{-1}. Each genotype has random values of α, β and τ within realistic ranges for phage ϕ6.

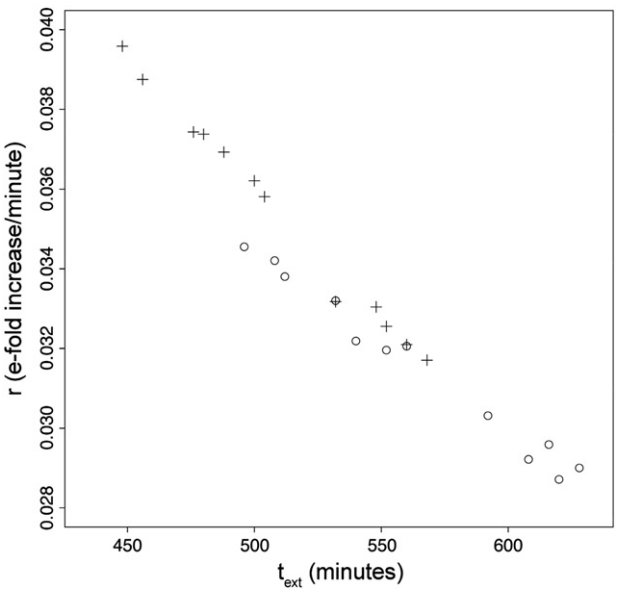

Fig. 4. Relationship between t_{ext} and realized rates of phage increase. r is the intrinsic rate of increase of each phage population, calculated using Eq. (5) and measured titers. Data symbolized as 'O' were obtained on the first day of assayed measurements, while those symbolized as '+' represent independent trials conducted on a second day.

bacterial growth in liquid culture, we showed that new information on virus attack could be extracted with high throughput. We developed a simple model to demonstrate that these growth curves of host bacteria correlated with known differences in relative fitness among genotypes of phage ϕ6.

Our new technique provides several advantages over classic plaque assays. In particular, the method allows viral isolates to be compared and contrasted efficiently and relatively inexpensively (e.g., compared to genetic sequence comparisons), given access to a microplate spectrophotometer. Thus, inter- and intra-population variation can be gauged quickly, as well as simultaneously on a single 96-well microplate. Such concurrent analysis is useful for minimizing potential block effects, such as stochastic differences among empirical replicates caused by assays performed on separate days. Furthermore, our analysis of changes in optical density through time provides a means for using this visual information to easily interpret how observed bacterial dynamics translate to differing growth success of lytic viruses. The resulting data can be used to convey new insights which would be difficult or impossible to discern from relatively more labor-intense methods, such as virus growth curves obtained through standard plaque assays.

An inevitable limitation of any fitness measurement is that the conclusions drawn from the measurement may be particular to a specific environment. Our results are highly promising because we compared phage genotypes in terms of their growth in liquid (an unstructured environment), and these results correlated strongly with absolute fitness (pfu per ml) rankings discerned through traditional plaque assays on agar (a structured environment). We note that this same relationship may not hold in other phage systems. However, we anticipate that in the future large-scale evolution experiments with phage will be conducted in small volumes housed in microplates, which will be amenable to automated dilution and propagation, such as using liquid-handling robotics. Thus, our method would provide an ideal assay for comparing growth of phages under these conditions, in which case the method itself would be identical to the conditions imposed during experimental evolution.

Evolutionary biologists have many good reasons to be fascinated by phages: they are elegant models to study the genetics of adaptation, challenging puzzles for phylogenetic analysis, ubiquitous agents of selection on bacteria, and convenient analogs of medically important disease agents such as Influenza-A Virus. Realizing this scientific potential requires new laboratory techniques that apply modern methods to answer questions relevant to evolution. This study adapts a relatively common microbiological tool, the spectrophotometer, to quantify the growth of phage, and applies it to studies with RNA phage ϕ6. Our goal is that the precision and efficiency of this method will help facilitate a new generation of larger, more statistically powerful evolution experiments harnessing phage.

Acknowledgments

We thank J. Shapiro and members of the Turner laboratory group for helpful comments on an early version of the manuscript. N. Morales provided excellent technical support. This work was supported by a National Aeronautics and Space Administration Graduate Research Fellowship to J.A.D.

Appendix A*A.1. Numerical simulations*

Our simulations calculate the state of the system at $t + \Delta t$ from the values of the variables at t and the previous values of I_t. Infected cells are binned into intervals of one second duration, and burst precisely τ minutes later. Simulations with variable burst times did not produce qualitatively distinct results. This numerical algorithm is essentially a first-order approximation, like Euler's method, and may therefore produce imprecise or unstable estimates of the variables (Strogatz, 1994). These errors can be reduced by decreasing the step size; however, round-off error, caused by the finite precision of digital computers, will increase as step size diminishes.

To manage these sources of error, our algorithm uses an adaptive step size. In practice, the $-\alpha SP$ term in Eqs. (1–3) is the most problematic. For example, this term can reduce S below zero when P is very large. Therefore, we use this term to tune the algorithm. In each iteration, the step size, Δt, is initially set to 6 s. Then, projected changes are calculated, and if $\Delta t \alpha SP$ is greater in magnitude than 10% of either P or S, the step size is halved repeatedly until neither condition holds.

This method produces smooth curves of $S(t)$ and prevents obvious anomalies, such as negative values for any variable. To estimate the significance of errors introduced by our numerical method, we performed two controls. To estimate the imprecision of our first-order approximation, we repeated the simulations shown in Fig. 1 with the rule that $\Delta t \alpha SP$ must be less than 20% of P and S. This modification should roughly double the step size when SP is large. The Pearson correlation between the original calculated r values, $r_{10\%}$, and these new values, $r_{20\%}$, was 0.9999996. This indicates that step sizes are sufficiently small to produce stable, precise estimates. We also repeated these simulations with a threshold of 1%. If round-off is a significant source of error, its effects should be magnified at these small step sizes. The correlation between $r_{10\%}$ and $r_{1\%}$ was 0.9999994, again indicating the robustness of our method.

References

Abedon, S.T., 1989. Selection for bacteriophage latent period length by bacterial density — a theoretical examination. Microb. Ecol. 18, 79–88.
Abedon, S.T., Herschler, T.D., Stopar, D., 2001. Bacteriophage latent-period evolution as a response to resource availability. Appl. Environ. Microbiol. 67, 4233–4241.
Abedon, S.T., Hyman, P., Thomas, C., 2003. Experimental examination of bacteriophage latent-period evolution as a response to bacterial availability. Appl. Environ. Microbiol. 69, 7499–7506.
Bull, J.J., 2006. Optimality models of phage life history and parallels in disease evolution. J. Theor. Biol. 241, 928–938.
Chao, L., 1990. Fitness of RNA virus decreased by Muller's ratchet. Nature 348, 454–455.
Crick, F.H.C., Leslie Barnett, F.R.S., Brenner, S., Watts-Tobin, R.J., 1961. General nature of the genetic code for proteins. Nature 192, 1227–1232.
Davis, R.H., 2003. The Microbial Models of Molecular Biology: From Genes to Genomes. Oxford University Press, New York.
Dennehy, J.J., Turner, P.E., 2004. Reduced fecundity is the cost of cheating in RNA virus ϕ6. Proc. R. Soc. Biol. Sci. 271, 2275–2282.
Dennehy, J.J., Abedon, S.A., Turner, P.E., 2007. Host density impacts relative fitness of bacteriophage ϕ6 genotypes in structured habitats. Evolution 61, 2516–2527.
Duffy, S., Turner, P.E., 2008. Introduction to phage evolutionary biology. In: Abedon, S.T. (Ed.), Bacteriophage Ecology: Population Growth, Evolution, and Impact of Bacterial Viruses. Cambridge University Press, Cambridge, pp. 147–176.
Froissart, R., Wilke, C., Montville, R., Remold, S., Chao, L., Turner, P.E., 2004. Co-infection weakens selection against epistatic mutations in RNA viruses. Genetics 168, 9–19 (Corrigendum: Genetics (2006) 172, 2705).
Hegreness, M., Shoresh, N., Hartl, D., Kishony, R., 2006. An equivalence principle for the incorporation of favorable mutations in asexual populations. Science 311, 1615–1617.
Heineman, R.H., Bull, J.J., 2007. Genetic constraint prevents adaptation to an optimal phenotype: experimental selection on lysis time in a phage. Evolution 61, 1695–1709.
Kenney, J.M., Hantula, J., Fuller, S.D., Mindich, L., Ojala, P.M., Bamford, D.H., 1992. Bacteriophage ϕ6 envelope elucidated by chemical cross-linking, immunodetection, and cryoelectron microscopy. Virology 190, 635–644.
McBride, R.C., Ogbunugafor, C.B., Turner, P.E., 2008. Robustness promotes evolvability of thermotolerance in an RNA virus. BMC Evol. Biol. 8, 231.
Montville, R., Froissart, R., Remold, S.K., Tenaillon, O., Turner, P.E., 2005. Evolution of mutational robustness in RNA viruses. PLoS Biol. 3 (11), 1939–1945.
Strogatz, S.H., 1994. Nonlinear Dynamics and Chaos. Perseus Books, New York.
Turner, P.E., Chao, L., 1998. Sex and the evolution of intrahost competition in RNA virus ϕ6. Genetics 150, 523–532.
Turner, P.E., McBride, R., Zeyl, C.W., 2009. Sexual exploits in experimental evolution. In: Garland Jr., T., Rose, M.R. (Eds.), Experimental Evolution: Concepts, Methods and Applications of Selection Experiments. University of California Press, Berkeley, pp. 479–521.
Wang, I.-N., 2006. Lysis timing and bacteriophage fitness. Genetics 172, 17–26.